ELSEVIER

Biochimica et Biophysica Acta 1564 (2002) 57–65

BIOCHIMICA ET BIOPHYSICA ACTA
BBA

www.bba-direct.com

Conformational transitions of membrane-bound HIV-1 fusion peptide

Asier Sáez-Cirión, José L. Nieva*

Unidad de Biofísica (CSIC-UPV/EHU) and Departamento de Bioquímica, Universidad del País Vasco, Aptdo. 644, 48080 Bilbao, Spain

Received 13 December 2001; received in revised form 12 March 2002; accepted 14 March 2002

Abstract

The human immunodeficiency virus type-1 (HIV-1) fusion peptide (FP) functions as a non-constitutive membrane anchor that translocates into membranes during envelope glycoprotein-induced fusion. Here, by means of infrared spectroscopy (IR) and of various bilayer-perturbation assays, we describe the peptide conformations that are accessible to its membrane-bound state and the transitions occurring between them. The peptide underwent a conformational transition from a predominantly α-helical structure to extended β-type strands by increasing peptide concentration in 1-palmitoyl-2-oleoylphosphatidylglycerol (POPG) vesicles. A comparable transition was observed at a fixed 1:100 peptide-to-lipid ratio when calcium was added to vesicles containing prebound α-helical peptide. Cation binding induced an increase in the amount of H-bonded carbonyls within the interfacial region of POPG. Calcium-promoted α → β conversion in membranes correlated with the closure of preformed lytic pores and took place in dispersed (nonaggregated) vesicles doped with poly(ethylene glycol)–lipid conjugates, showing that the conformational transition was independent of vesicle aggregation. We conclude that the target membrane conditions modulate the eventual structure adopted by the HIV-1 FP. Conformational polymorphism of the inserted peptide may contribute to the flexibility of the fusogenic complex during the fusion reaction cycle, and/or may be related to target membrane perturbation at the fusion locus.

Keywords: Membrane fusion; Viral fusion; HIV-1; Fusion peptide; Peptide–lipid interaction; Peptide conformation

1. Introduction

In human immunodeficiency virus type-1 (HIV-1), the approximately 25 amino acid-long fusion peptide (FP) is located at the N-terminus of the gp41 transmembrane subunit of the envelope protein [1,2]. Current models postulate that this long hydrophobic and conserved region represents an additional membrane domain that transfers into the target cell membrane during gp41-mediated fusion [3,4]. Mutational analysis supports direct involvement of FP in the fusion reaction [5–7]. Important sequence features related to function include the presence of the LFLGFL interfacial segment, probably involved in promoting spontaneous transferring into target membranes, and the occurrence of six Gly and five Ala residues which suggests an intrinsic high degree of conformational plasticity [1,8–10].

Conformational flexibility is not unexpected given the different folding states that HIV-1 FP is presumed to adopt during gp41-mediated fusion. The prevailing hypothesis states that HIV-1 fusion cascade starts when a gp120 surface subunit interacts with receptor and coreceptors (for recent reviews, see: Refs. [3,4,11]). During the process, the transmembrane gp41 subunit undergoes structural rearrangements, notably the formation and/or reorientation of a triple-stranded α-helical coiled-coil domain, thought to bring about exposure of the previously cryptic FP in the vicinity of the target membrane. The intermediate structure connecting viral and target cell membranes would subsequently act as a collapsible device that would reorganize into a six-helix bundle, or trimeric hairpin, and eventually juxtapose coupled

Abbreviations: ANTS, 8-aminonaphtalene-1,3,6-trisulfonic acid sodium salt; Chol, cholesterol; DMSO, dimethylsulfoxide; DNS-DHPE, *N*-(5-dimethylaminonaphtalene-1-sulfonyl)-1,2-dihexadecanoyl-*sn*-glycero-3-phosphoethanolamine; DPX, *p*-xylenebis(pyridinium)bromide; DOPC, dioleoylphosphatidylcholine; DOPE, dioleoylphosphatidylethanolamine; FP, fusion peptide; HIV, human immunodeficiency virus; IR, infrared spectroscopy; LUV, Large unilamellar vesicles; N-NBD-PE, *N*-(7-nitrobenz-2-oxa-1,3-diazol-4-yl)phosphatidylethanolamine; N-Rho-PE, *N*-(lissamine Rhodamine B sulfonyl)phosphatidylethanolamine; PC, phosphatidylcholine; PEG-PE, distearoylphosphatidylethanolamine-poly(ethylene glycol); POPG, 1-palmitoyl-2-oleoylphosphatidylglycerol; THF, tetrahydrofurane

* Corresponding author. Departamento de Bioquímica, Universidad del País Vasco, Aptdo. 644, 48080 Bilbao, Spain. Tel.: +34-94-6012615; fax: +34-94-4648500.

E-mail address: gbpniesj@lg.ehu.es (J.L. Nieva).

0005-2736/02/$ - see front matter
PII: S0005-2736(02)00400-5

membranes. Thus, according to this mechanism, the FP sequence would (a) be initially folded as a part of the gp41 ectodomain globular structure, (b) then be transiently exposed to water at the tip of the triple stranded coiled-coil, (c) afterwards be inserted as an anchor into the target membrane, and (d) finally form an active part of a fusogenic complex that perturbs bilayers to open a fusion pore.

The ability of the HIV-1 FP sequence to adopt different structures has been confirmed by numerous experiments using synthetic sequences and model membranes (reviewed in: Refs. [8–10], see also: Ref. [12]). We described a system consisting of negatively charged 1-palmitoyl-2-oleoylphosphatidylglycerol (POPG) vesicles, in the presence or absence of divalent cations, as targets for the FP [13]. In that previous work, we reported independent evidence for peptide-induced mixing of bilayer lipids, for mixing of aqueous vesicle contents, and for the occurrence of an irreversible increase in vesicle size. To observe fusion induced by the peptide, divalent cations were required in the medium. We caution that divalent cations alone did not induce any vesicle fusion in the concentration range used in those studies. Our experimental approach further allowed the assignment of distinct membrane-bound peptide structures to specific perturbations. In the absence of cations, leakage of contents was promoted by peptides adopting an α-helical conformation, whereas fusion was promoted in the presence of cations by extended β-strands [13,14]. The latter structure was afterwards shown to be prevalent in electrically neutral dioleoylphosphatidylcholine (DOPC): dioleoylphosphatidylethanolamine (DOPE):cholesterol (Chol) vesicles, even in the dispersed unfused liposomes containing low peptide doses [15]. For comparison, using identical sample preparation protocols, we found mainly α-helix in pure POPG liposomes at 1:65 peptide-to-lipid ratio [13], and mainly β-strand in neutral DOPC:DOPE:Chol vesicles at 1:800 peptide-to-lipid ratio [15]. Infrared reflection–absorption spectroscopy data confirmed the adoption by the peptide of a main β-sheet structure in a single monolayer of neutral lipids [16]. Therefore, adoption of a particular conformation seemed to depend on the nature of the membrane matrix rather than on artefactual production by peptide dose or membrane aggregation.

Recent solid-state nuclear magnetic resonance (SS-NMR) results by the group of Weliky [12] provide new experimental evidence for an extended β-strand conformation of the membrane-bound HIV-1 FP under fusion-inducing conditions. These authors found that the N-terminal and central regions of the peptide were well structured as β-strands in membranes composed of a lipid mixture mimicking target T-cell membranes. Vesicles composed of that mixture were readily fused by the peptide under the SS-NMR measuring conditions. Thus, the findings in that work further emphasize the putative functional relevance of the extended peptide structure.

In the present study, we report on an important observation, namely the conversion of membrane-bound HIV-1 FP α-helices into β-strands. Conversion occurs after increasing peptide loads in membranes, but also at a fixed low peptide dose after addition of calcium. We exploit this latter effect to further investigate the possible relevance in HIV-1 fusion of the different FP membrane structures. Our results support the notion that the HIV-1 FP is conformationally polymorphic in dispersed membranes, a property susceptible to be modulated by bilayer conditions such as surface compression or polar head group conformation. This observation may be of physiological relevance if, as proposed, intrinsic monolayer curvatures change during the fusion reaction mediated by gp41.

2. Materials and methods

N-(7-nitrobenz-2-oxa-1,3-diazol-4-yl)phosphatidylethanolamine (N-NBD-PE), *N*-(lissamine Rhodamine B sulfonyl)phosphatidylethanolamine (N-Rho-PE), distearoylphosphatidylethanolamine-poly(ethylene glycol) [MW of poly(ethylene glycol) ~2000] (PEG-PE) and 1-palmitoyl-2-oleoyl-phosphatidylglycerol (POPG) were purchased from Avanti Polar Lipids (Birmingham, AL, USA). *N*-(5-dimethylaminonaphtalene-1-sulfonyl)-1,2-dihexadecanoyl-*sn*-glycero-3-phosphoethanolamine (DNS-DHPE), 8-aminonaphtalene-1,3,6-trisulfonic acid sodium salt (ANTS) and *p*-xylenebis(pyridinium)bromide (DPX) were from Molecular Probes (Junction City, OR, USA). Tetrahydrofurane (THF), D_2O and Triton X-100 were obtained from Sigma (St. Louis, MO, USA). All other reagents were of analytical grade. The sequence representing the N-terminus of the HIV gp41, HIV-1 FP, AVGIGALFLGFLGAAGSTMGARS and its fluorescent derivative containing the F8W substitution were synthesized as their C-terminal carboxamides and purified (estimated homogeneity >90%) by Quality Controlled Biochemicals (Hopkinton, MA, USA). Peptide stock solutions were prepared in dimethylsulfoxide (DMSO, spectroscopy grade).

Large unilamellar vesicles (LUV) were prepared according to the extrusion method of Hope et al. [17] in 5 mM Hepes, 100 mM NaCl (pH 7.4). Lipid concentrations of liposome suspensions were determined by phosphate analysis [18]. Mean diameter of vesicles was 120 nm as estimated by quasielastic light scattering using a Malvern Zeta-Sizer instrument.

Release of vesicular contents to the medium was monitored by the ANTS/DPX assay. LUV containing 12.5 mM ANTS, 45 mM DPX, 20 mM NaCl and 5 mM Hepes [19] were obtained by separating the unencapsulated material by gel filtration in a Sephadex G-75 column eluted with 5 mM Hepes, 100 mM NaCl (pH 7.4). Osmolarities were adjusted to 200 mosM in a cryoscopic osmometer (Osmomat 030, Gonotec, Berlin, Germany). Fluorescence measurements were performed by setting ANTS emission at 520 nm and excitation at 355 nm. A cutoff filter (470 nm) was placed between the sample and the emission monochromator. 0%

leakage corresponded to the fluorescence of the vesicles at time zero; 100% leakage was the fluorescence value obtained after addition of Triton X-100 (0.5% v/v).

Entry of solutes into vesicles was evaluated, through the selective reduction of the NBD probe residing in the inner leaflet of vesicle membranes, according to the method described by McIntyre and Sleight [20]. Vesicles symmetrically labeled with N-NBD-PE (0.6 mol%) were incubated with peptide for 30 min. Then dithionite (10 mM) was added to peptide–vesicle mixtures. Degree of vesicle permeabilization was inferred comparing the percentage of reduced NBD in peptide-treated and untreated vesicles. Percentage of NBD reduction was calculated following the equation:

$$\% \text{ Reduced NBD} = [(F_f - F_0)/(F_{100} - F_0)] \times 100 \quad (1)$$

where F_0 corresponds to the NBD fluorescence value after dithionite addition to untreated vesicles, F_f is the final fluorescence after incubation with peptide and dithionite, and F_{100} is the fluorescence value of solubilized vesicles incubated with dithionite.

Membrane lipid mixing was monitored using the resonance energy transfer (RET) assay, described by Struck et al. [21]. The assay is based on the dilution of N-NBD-PE and N-Rho-PE. Dilution due to membrane mixing results in an increase in N-NBD-PE fluorescence. Vesicles containing 0.6 mol% of each probe were mixed with unlabeled vesicles at 1:4 ratio. The NBD emission was monitored at 530 nm with the excitation wavelength set at 465 nm. A cutoff filter at 515 nm was used between the sample and the emission monochromator to avoid scattering interferences. The fluorescence scale was calibrated such that the zero level corresponded to the initial residual fluorescence of the labeled vesicles and the 100% value to complete mixing of all the lipids in the system. The latter value was set by the fluorescence intensity of vesicles, labeled with 0.12 mol% each of the fluorophores, at the same total lipid concentration as in the fusion assay.

Fluorescence energy transfer from peptide–Trp to the surface fluorescent probe DNS-DHPE was measured as in Refs. [22,23]. 6.25 mol% of DNS-DHPE probe was included in the target vesicle composition (0.25 mM). Lipid–peptide mixtures were incubated at room temperature for 30 min before data acquisition. Corrected spectra were recorded in a Perkin Elmer LS-50B spectrofluorimeter with excitation set at 280 nm and slits of 5 nm for both excitation and emission. The efficiency of energy transfer (E) was determined according to Stryer [24] from the relative fluorescence intensity of the Trp in the absence (Q_0) and presence (Q_T) of DNS-DHPE in the vesicles as:

$$E = 1 - (Q_T/Q_0) \quad (2)$$

Specific labeling of bilayer outer-leaflets was accomplished as described in Ref. [23]. Briefly, vesicles were incubated for 15 min with externally added DNS-DHPE (3.75 mol% with respect to total lipid in vesicles) from a THF solution (5 mM). Further exchange of external buffer at 4 °C through gel filtration on a Sephadex G-75 column rendered vesicles asymmetrically labeled in their external monolayer with the fluorescent DNS probe.

Infrared spectroscopy (IR) measurements were conducted essentially as described in Refs. [13–15]. Membrane samples consisted of floated peptide–lipid complexes obtained after ultracentrifugation in D_2O buffer. Solvent samples were also obtained from the supernatant fraction not containing lipid or peptide and subsequently used as background controls. Infrared spectra were recorded in a Nicolet 520 spectrometer equipped with an MCT detector. Samples were placed between two CaF_2 windows separated by 50 μm spacers. One thousand scans (sample) and 1000 scans (reference) were taken for each spectrum, using a shuttle device. Spectra were transferred to a computer where solvent subtraction and band-position determinations were performed using GRAMS software (Galactic) as previously reported [25].

3. Results

The HIV-1 FP was previously shown to exist in POPG membranes in predominantly α or β conformations, according to the experimental conditions [2,13]. In the present work, we have used an analog that contains a Trp residue replacing Phe in position 8 and retains its full fusogenic capacity [16]. The presence of the Trp residue allowed a direct estimation of the peptide doses in the membrane under our experimental conditions. To verify that this variant reproduced an equivalent conformational behavior in solution and in POPG membranes, its structures were determined by means of IR. Similarly to the parental HIV-1 FP sequence, the F8W analog peptide adopted a main extended conformation in solution, an α-helical structure in pure POPG vesicles, and again β-like extended strands when the latter vesicles were preincubated with 5 mM calcium before peptide addition (data not shown).

Thus, the intrinsically fluorescent variant was a suitable tool to investigate the parameters that govern the adoption of different structures by the HIV-1 FP, since it allowed simultaneous monitoring of structure and peptide dose in the membrane. This was particularly useful to infer the effect of increasing peptide doses on the structures adopted by the peptide in POPG LUV. Gp41-mediated fusion is postulated to occur within defined spots of the interacting membranes, as promoted by preformed high-order complexes [26]. Therefore, it has been proposed that in this physiological situation, the local concentration of inserted FPs in the target membrane is relatively high [10]. As shown by IR spectra in Fig. 1A, increasing peptide loads in POPG LUV correlated with an increment in the amide-I peak corresponding to aggregates of extended structure. Note that the samples had been freed from unbound peptide by centrifugation (flota-

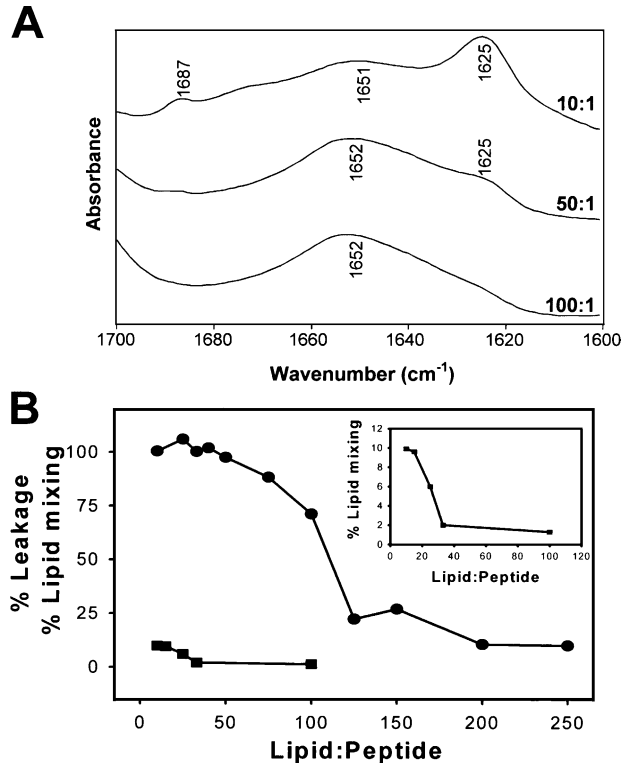

Fig. 1. Structures adopted by HIV-1 FP (F8W analog) and induced POPG membrane perturbations as a function of the peptide dose. (A) IR spectra of the peptide bound to POPG vesicles at increasing peptide-to-lipid ratios. (B) Final extents of leakage (circles) and intervesicular lipid mixing (squares) as a function of peptide to lipid mole ratio. Lipid concentration was constant (100 μM). Inset: extents of lipid mixing at the highest peptide-to-lipid ratios tested.

tion) before the spectroscopic measurements (see Materials and Methods). These results are consistent with former IR data obtained by Rafalski et al. [2] and Mobley et al. [27] in dried and dried-wetted multilayers, respectively. The leakage and intervesicular lipid mixing results shown in Fig. 1B revealed certain activation of the latter process only at the highest loads tested (>1:30 peptide/lipid mole ratios), whereas vesicles were efficiently permeabilized at 1:100 peptide-to-lipid ratio where almost pure helical conformation was observed (see also Table 1).

Table 1
Main IR band components and adopted secondary structures by HIV-1 FP associated to POPG vesicles

Sample (lipid:peptide)[a]	Main peaks (wavenumber, cm^{-1})	Main structures
10:1	1625, 1651, 1687	α-helix, β-sheet
50:1	1652	α-helix
100:1	1652	α-helix
100:1 + Ca^{2+}	1626, 1652, 1688	α-helix, β-sheet
100:1 (Ca^{2+})	1625, 1687	β-sheet
100:1 PEG-PE	1651	α-helix
100:1 PEG-PE (Ca^{2+})	1626, 1687	β-sheet

[a] "+Ca^{2+}" indicates that the cation was added to preformed peptide–vesicle complexes (final concentration, 5mM) while "(Ca^{2+})" corresponds to samples containing 5 mM calcium before the addition of peptide. "PEG-PE" indicates that vesicles contained this lipid at 5 mol% concentration.

The high peptide loads required in POPG LUV to promote the α→β conformational transition make difficult any clear distinction between localized membrane perturbations, specifically induced by the FP sequence, and unspecific processes due to peptide-mass transfer to the membrane. For instance, at extremely high peptide concentrations, lipids might exchange between aggregated vesicles through processes other than fusion. This fact prompted us to explore the ability of calcium to induce a similar transition in situ at the low peptide doses at which the helical conformation was predominant. To that end, we first characterized the structural effect of adding the cation to preincubated peptide–lipid mixtures (Fig. 2). We note that in comparison to the experimental protocols used in previous works [13,14], this was a new condition in the sense that here we explored the effect of calcium added to peptides prebound to POPG LUV, that is, already in an α-helical structure. The spectra displayed in Fig. 2A, obtained before

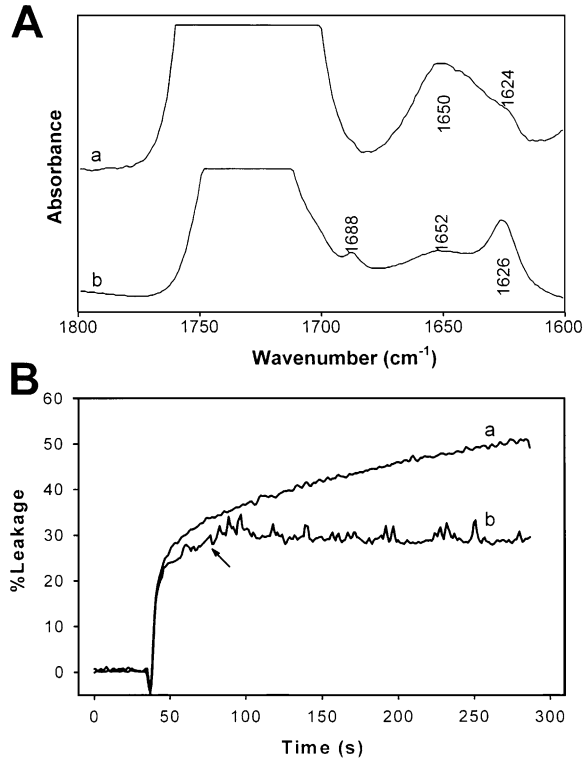

Fig. 2. Conformational transition induced by addition of calcium on HIV-1 FP bound to POPG LUV. (A) IR spectra of the peptide bound to POPG vesicles. Curve a: Peptide and vesicles were incubated for 30 min at a peptide-to-lipid ratio of 1:100, before being subjected to flotation in D_2O buffer. Curve b: Peptide and vesicles were incubated for 30 min at a peptide-to-lipid ratio of 1:100 and then calcium was added (final concentration, 5 mM). The mixture was further incubated for 30 min before flotation. (B) Inhibition of FP-induced leakage by calcium. Leakage was measured as a function of time (a). In curve (b), the cation (final concentration, 5 mM) was added at the time indicated by the arrow. Peptide-to-lipid ratio was 1:100.

and after calcium addition, demonstrated the existence of an α→β conformational transition. Peptide membrane-loads in both samples were simultaneously determined as described [16]. In accordance with results reported by Mobley et al. [27], we found that the peptide bound almost quantitatively to POPG LUV under our experimental conditions. Moreover, the initial membrane peptide-load did not appreciably change in the presence of the cation (not shown). Thus, the observed conformational transition occurred in membranes at invariant peptide concentration. Data in panel B demonstrate that calcium addition also arrested the ongoing leakage process induced by the peptide, suggesting that the conformational transition to the β-type structure causes the inhibition of pore formation. The fast effect of calcium on the process suggests that the transition occurred almost simultaneously to binding of the cation by the phospholipid.

IR provides useful information on Ca^{2+}-induced conformational changes in phospholipids [28–30]. In particular, the carbonyl stretching vibrations [31], report on the conditions in the membrane–water interface region. The spectrum of pure POPG dispersed in D_2O buffer (Fig. 3A) shows that the carbonyl stretching region (1800–1700 cm^{-1}) was composed of two bands centered at 1743 and 1725 cm^{-1}, corresponding to non-hydrogen bonded and monohydrated carbonyl groups, respectively [31]. Addition

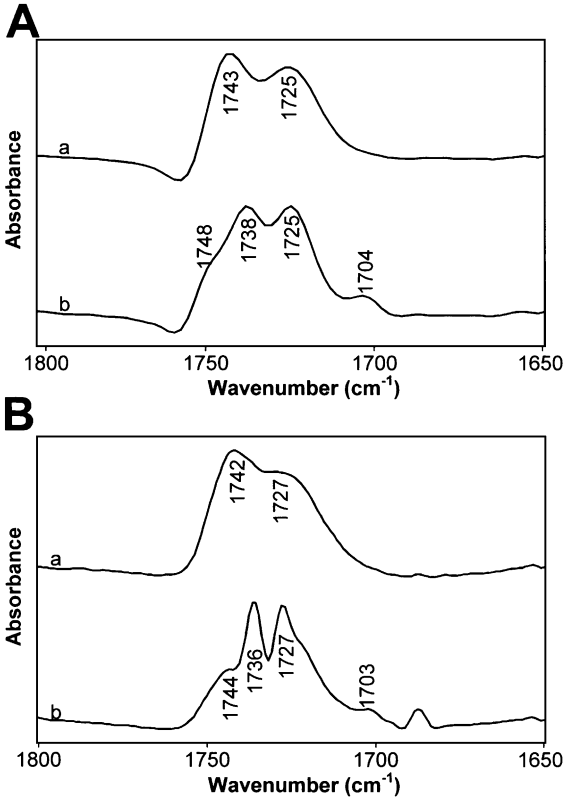

Fig. 3. Infrared Fourier self-deconvoluted spectra of POPG in the C═O stretching region. (A) Multilayers hydrated in D_2O buffer: (a) pure POPG; (b) POPG–calcium. (B) Floated peptide–POPG LUV complexes: (a) in the absence of calcium; (b) in the presence of 5 mM calcium.

of calcium to these samples induced the appearance of new and narrower component bands, centered at 1738 and 1725 cm^{-1}, most likely arising from the phospholipid population interacting with the cation. In addition, a lower frequency band at 1704 cm^{-1} became evident. The latter vibration has been assigned to C═O groups forming hydrogen bonds with two molecules of water [31]. Parallel spectra in panel B show that, in the absence of calcium, the carbonyl stretching bands in the peptide–lipid complexes isolated by flotation were similar to those observed in hydrated POPG samples. In presence of the cation, floated peptide–lipid complexes showed sharp 1736 and 1727 cm^{-1} components together with the lower frequency 1703 cm^{-1} band.

The shift of ~6 cm^{-1} in the maximum absorbance of the dehydrated carbonyl groups suggests the existence of a conformational change induced by calcium in the interfacial region of POPG. Moreover, the band narrowing in the presence of the cation would be consistent with a higher degree of immobilization in this configuration. This effect is comparable to the one observed in phosphatidylserine membranes where calcium has been shown to induce a rigid conformation of the carbonyls, even though these moieties remain hydrated [28–30]. The change induced by calcium in the POPG system also resulted in a relative increase of the monohydrated carbonyls (1727 cm^{-1}) with respect to dehydrated species (1736 cm^{-1}). This fact together with the appearance of disolvated species (1703 cm^{-1}) suggests a higher degree of hydrogen-bonded C═O groups in cation-treated samples.

The calcium-induced changes were not only affecting the peptide before the assembly of POPG-embedded pores (Fig. 2B), but could also act on preformed pores. This was shown in experiments in which the closure of preformed pores was investigated in fully permeabilized vesicles. The latter were obtained by incubating POPG LUV with a peptide dose inducing 100% leakage (Fig. 4A). Further size-distribution determination indicated that untreated and permeabilized vesicles had the same average size. To assay solute entry into these vesicles, we measured the percentage of NBD reduction in POPG/NBD-PE (99.4:0.6 mole ratio) by externally added dithionite. In symmetrically labeled vesicles, this compound reduced approximately 60% of NBD as judged from the decrease in fluorescence intensity (Fig. 4B), indicating specific reduction of the probe residing in the external membrane leaflet [20]. Thus, we considered this value as the zero level of entry, whereas complete reduction in solubilized vesicles was taken as the 100% value. Full permeabilization of vesicles treated with peptide as in panel A was evidenced from the capacity of dithionite to reduce 100% of the NBD in these samples (curve b in panel B). Data in Fig. 4C are consistent with almost complete inhibition of solute entry by preincubation of permeabilized vesicles with calcium. Moreover, addition of the cation in the midst of solute entry arrested the process. We conclude that HIV-1 FP pores established in POPG LUV may close after addition of calcium.

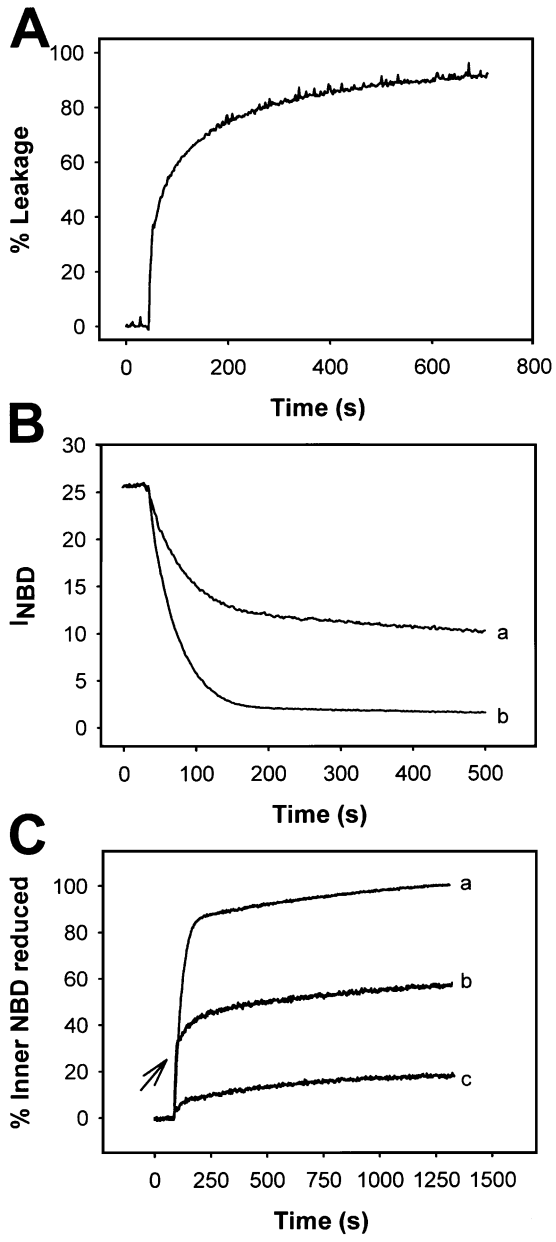

Fig. 4. Closure of preformed HIV-1 FP pores after addition of calcium. (A) Peptide-induced leakage of POPG vesicles (ANTS/DPX assay) as a function of time. The peptide-to-lipid ratio was 1:25. (B) NBD reduction by dithionite. Curve a: POPG:NBD-PE vesicles treated with dithionite (added at time=60 min); curve b: POPG:NBD-PE vesicles preincubated with the peptide for 1 h under conditions in panel A, and then treated with dithionite. (C) Entry of solutes (dithionite assay) into permeabilized POPG vesicles. Vesicles were incubated with the peptide for 1 h (conditions as described in panel A) before dithionite addition. Curve a: permeabilized POPG:NBD-PE vesicles; curve b: calcium (final concentration, 5 mM) was added after dithionite at the time indicated by the arrow; curve c: permeabilized POPG:NBD-PE vesicles incubated with 5 mM calcium before dithionite addition.

Vesicle aggregation had no effect on the conformational transition, that is, the transition could develop in isolated liposomes. This was demonstrated by using polyethylene glycol-grafted POPG vesicles. PEG moiety has been demonstrated to act as a steric barrier that hinders bilayer–bilayer contacts [32,33]. We used a polymer containing 45 ethylenes per unit (MW ~ 2000) which depending on its density may project from 35 to 160 Å from the bilayer surface [34]. When this compound was included in the liposome formulation, the capacity of the HIV-1 FP to induce intervesicular lipid mixing in the presence of calcium was inhibited (Fig. 5). Peptide-induced mixing of membranes was reduced by more than 50% when the liposomes contained 1 mol% PEG-PE, and 5 mol% PEG-PE arrested the process almost completely. The lipid mixing levels detected under the latter conditions were even below those detected in the absence of calcium. Control experiments demonstrated that peptide doses in the membrane did not change after inclusion of PEG-PE. Moreover, determination of vesicle size distributions showed that the mean diameter did not change appreciably. Thus, in POPG/PEG-PE (95:5 mole ratio) vesicles, the peptide capacity to induce aggregation and fusion was inhibited.

In contrast, the peptide efficiently permeabilized those vesicles (Fig. 6). Results in Fig. 6A demonstrate that the peptide induced leakage from POPG/PEG-PE (95:5 mole ratio) and POPG LUV to comparable levels. But even more important, in the presence of calcium, leakage was similarly reduced in both types of vesicles indicating that the cation interfered with this process independently of the induction of membrane aggregation and/or fusion. Results in panel B reflect that addition of calcium also arrested ongoing leakage in POPG/PEG-PE (95:5 mole ratio) LUV, a fact consistent with a structural transition taking place in these dispersed bilayers. IR actually confirmed the existence of the $\alpha \rightarrow \beta$ structural transition in POPG/PEG-PE (95:5 mole ratio) membranes (Table 1). The peptide bound to POPG/PEG-

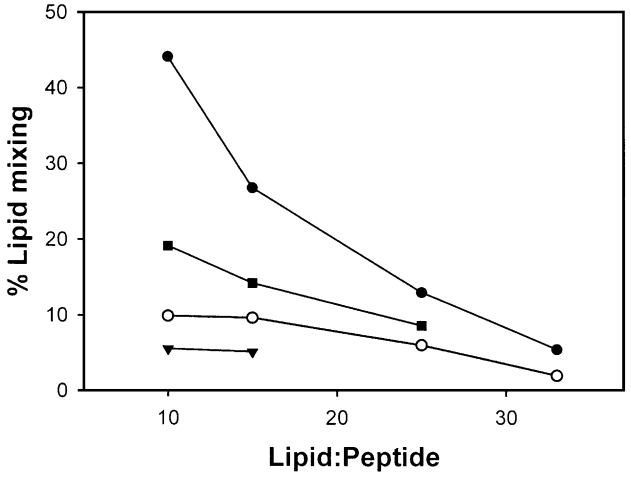

Fig. 5. Intervesicular mixing of lipids induced in presence of 5 mM calcium by the HIV-1 FP. POPG (filled circles), POPG:PEG-PE (99:1 mole ratio) (squares) and POPG:PEG-PE (95:5 mole ratio) (inverted triangles). Empty circles correspond to the FP effect in POPG vesicles in the absence of calcium. Final extents of the process were plotted as a function of the lipid-to-peptide ratio. Lipid concentration was fixed to 100 μM in all cases.

PE vesicles showed a main IR absorption band at 1651 cm^{-1} that converted into 1626 and 1687 cm^{-1} upon addition of calcium to mixtures, consistent with mainly α-helical and extended structures before and after addition, respectively. Of note, the observation of leakage in the presence of calcium in the dispersed POPG/PEG-PE vesicles (Fig. 6A), at the doses at which membrane mixing was detected in pure POPG vesicles, further supports the notion introduced in previous works [15,35] that the β-type structure may induce a type of membrane perturbation that causes permeabilization in isolated vesicles, but also their subsequent aggregation and fusion. In summary, results in Fig. 6 suggest that calcium promoted the α→β structural transition of the peptide by altering the conditions of the isolated bilayers and not through the induction of interbilayer contacts.

Moreover, experimental results in Fig. 7 show that calcium induced a superficial location of the peptide. The locations of the helical and extended conformations in the POPG bilayer were investigated through resonance energy transfer of the Trp-8 residue to the surface-residing dansyl moiety of the DNS-DHPE probe [22]. As shown in Fig. 7, both peptide conformations transferred energy to DNS-DHPE in symmetrically labeled LUV rather effectively [transfer efficiency (E) was 0.55 at 1:100 peptide/lipid ratio]. In comparison, when LUV were asymmetrically labeled in the outer-leaflet, energy transfer by the α-helical conformation was very much reduced (E = 0.1 at 1:100 peptide/lipid ratio) while the β-type structure was almost equally good as donor (E = 0.38 at 1:100 peptide/lipid ratio). The dansyl moiety of DNS-DHPE is located at the edge of the lipid–water interface in the vesicles [36]. The R_0 distance calculated for the dansyl–Trp couple is approximately 17 Å [37]. Assuming a bilayer thickness of 50 Å, the low energy transfer observed for the α-helical conformation in asymmetrically labeled LUV is likely to arise from a distant location of the Trp residue from the outer monolayer interface, a fact consistent with the deep penetration of the N-terminal section of the peptide [38]. In contrast, the comparable E values in both types of LUV observed for the β-type structure is consistent with an interaction mostly restricted to the outer membrane monolayer [16].

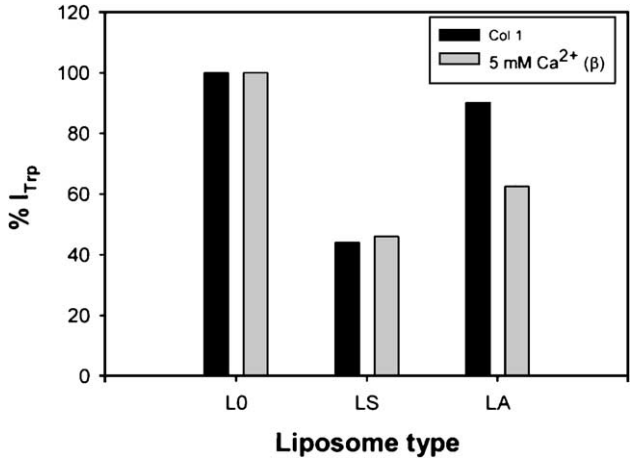

Fig. 7. Intrinsic fluorescence of FP analog containing a F8W substitution interacting with unlabeled POPG vesicles (L0), and POPG vesicles labeled with DNS-PE in both membrane leaflets (LS) or specifically in the external leaflet (LA). Experiments were carried out in presence and absence of 5 mM calcium as indicated in the panels. Peptide-to-lipid ratio was 1:100 and lipid concentration 100 μM in all measured samples.

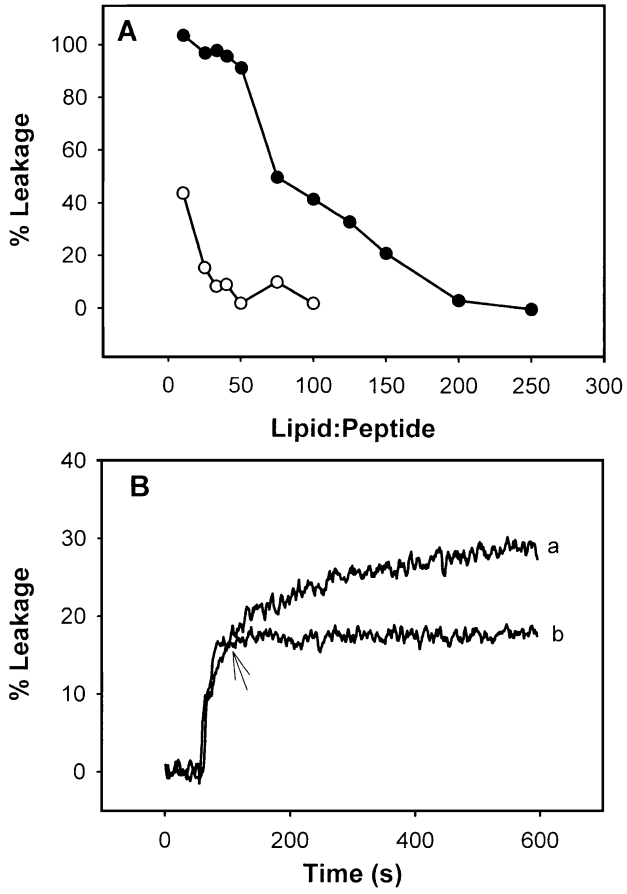

Fig. 6. Leakage of vesicular contents (ANTS/DPX assay) induced by the FP in POPG:PEG-PE (95:5) vesicles. (A) Final extents of the process as a function of the lipid-to-peptide ratio. Filled and empty circles correspond to experiments done in the absence and the presence (5 mM) of calcium, respectively. (B) Kinetics of leakage at 1:100 peptide-to-lipid ratio. In curve b, calcium was added at the time indicated by the arrow.

4. Discussion

In this work, we describe two factors that modulate the conformations accessible to the HIV-1 FP associated to POPG membranes, that is, peptide load and cation binding. The peptide adopted a stable helical conformation that could be converted into an extended β-type structure by addition of calcium. The use of intrinsically fluorescent peptide analogs allowed us to determine that the latter process occurred without a change in the amount of peptide bound

to membranes. Importantly, the cation-driven structural transition was observed to proceed in dispersed PEG-PE/POPG vesicles. We conclude that FP may exist in β-structures in isolated membranes and that these structures may perturb bilayers and induce in them a state of fusogenicity. Nevertheless, it should be pointed out that the model system described here is still far from reflecting entirely the in vivo complexity of the studied interaction, and that it should be rather considered as a tool useful to get insights into the structural behavior of the HIV-1 FP associated to membranes.

4.1. FP membrane dose and adopted conformations

The dose-dependent conformational polymorphism of HIV-1 FP in POPG membranes was first suggested by Rafalski et al. [2] in dried multilayers. These authors found that α-helical conformation and β-type structures predominated at 1:200 and 1:30 peptide-to-lipid ratios, respectively. At a peptide-to-lipid ratio of 1:17, the peptide was able to fuse POPG SUV (25% intervesicle lipid mixing). Our data in this work confirm that also when the peptide was incorporated from the aqueous phase into POPG LUV, increasing amounts in the bilayer resulted in an increased relative amount of β-structure adopted by FP (Fig. 2 and Table 1). The peptide also induced a certain amount of interLUV mixing of lipids at the highest peptide-to-lipid ratios tested (e.g., 10% at a 1:15 ratio). The higher levels of lipid mixing detected in SUV as compared to LUV probably reflect the intrinsic metastability of the former [39]. From our data, we may conclude that there exists a correlation between the ability of the HIV-1 FP to induce POPG LUV fusion and the dose-dependent accumulation of β-type structure. The same trend seems as well to operate in other lipid systems as inferred from published data (reviewed in Ref. [9]).

4.2. Membrane conditions and adopted conformation

The presence of a β-type structure is required for induction of fusion but it is not sufficient by itself. Rafalski et al. [2] showed that the HIV-1 FP adopted an extended structure in POPC membranes but was unable to fuse SUV composed of this lipid. These authors interpreted the requirement of POPG in this system as an indication of the FP helical structures being involved in fusion. However, we note that at the peptide-to-lipid ratios used in those experiments (1:17), the FP also adopted a predominantly β-type structure in POPG membranes . Therefore, it seems more likely that fusogenicity of the same β-type peptide may be modulated by the conditions in the membrane. In fact, inclusion into phosphatidylcholine (PC) membranes of phosphatidylethanolamine and cholesterol results in the induction of 100% LUV fusion by the peptide [15]. In this latter system, the adopted structure is extended for peptide-to-lipid ratios ranging between 1:800 and 1:10. Two main interrelated membrane factors may affect fusogenicity by the peptide. First, the intrinsic tendency of juxtaposed bilayers to fuse is modulated by the presence of non-lamellar lipids such as phosphatidylethanolamine with negative spontaneous curvature [40]. Second, the fact that the latter kind of lipids has a large apolar portion relative to their polar moiety (cone-like lipids), may facilitate access of the FP sequences to the interfacial region of the membrane (discussed in Ref. [41]). These assumptions are also supported by recent SS-NMR spectroscopy results by Yang et al. [12], indicating a greater structural order of the membrane-bound β-strand in lipid mixtures mimicking target T-cell plasma membrane. These authors found little dependence of structural distribution on peptide-to-lipid ratios for samples made of mixtures of lipids containing phosphatidylethanolamine and cholesterol, but a significant dependence in a sample made of a single lipid.

A parallel line of evidence comes from the use of cations to modulate POPG properties [13,14]. We found that under conditions where the peptide was able to induce substantial POPG LUV permeabilization, the adopted conformation in membranes was mainly helical and no fusion was detected. Addition of calcium to these samples caused closure of pores and a conformational transition towards a predominantly extended structure. Noteworthy, at peptide membrane-doses inducing permeabilization as an α-helix, for example, 1:100 peptide-to-lipid ratio, the extended structures formed after calcium addition showed no capacity to perturb membranes. These latter structures required higher doses of peptide in the membrane to perturb the bilayer architecture. Moreover, according to our results, the extended structures formed in dispersed (i.e., non-aggregated) membranes were primarily lytic (see also, Refs. [15,35]). Thus, the type of perturbation induced by the extended structure at higher doses seems to be qualitatively different from the one induced by the helical conformation. While the former compromises the overall bilayer organization causing permeabilization and further allowing the intermembrane mixing of constituent lipids, the latter establishes discrete structures through which solutes can cross the membrane in both directions.

The effect of calcium on POPG appears to be relatively similar to that caused by this cation on phosphatidylserine membranes [28–30]. Calcium binding induces a change in the polar head group conformation that becomes more rigid [29,30] and a differential reduction of the polar head group cross-sectional area [42], which may facilitate intrusion of water molecules through the interfacial region of the membrane. We propose that cation binding to POPG promotes the α→β conformational transition of HIV-1 FP as a consequence of its effects on the interfacial region of the membrane. The superficial location of the peptide (Fig. 7) might be favored by a head-group displacement similar to that produced in systems containing non-lamellar lipids [41]. In addition, the overall increase in hydrogen bonding (Fig. 6) might better satisfy the stability requirements of β-type strands immersed in the bilayer interface.

4.3. Relevance for HIV-1 fusion

HIV-1 FP may exist in bilayers in one of two main conformations, that is, lytic α-helices or interfacial β-strands, depending on conditions such as peptide-to-lipid ratio, membrane lipid composition, or concentration of divalent cations. This conformational polymorphism may be physiologically relevant. We envisage two non-mutually exclusive hypotheses to explain the importance of peptide plasticity in the gp41-mediated fusion process.

(1) Conformational polymorphism of the inserted HIV-1 FP might contribute to the flexibility of the fusogenic complex during the fusion reaction cycle if, as suggested by the ''hairpin'' model, the rod-shaped gp41 ectodomain goes from a conformation in which its axis is perpendicular to the target bilayer normal (inserted prefusion state or ''pre-hairpin'') to a conformation that is mainly parallel to the membrane interface (''hairpin'' structure) [3,4,11]. The intrinsic assumption within this model is that the FP behaves as a flexible anchor that alternates conformation and level of insertion in the membrane.

(2) Adoption of two conformations might also be related to induction of important membrane perturbations. Lytic helical structures might form within the target membrane as recently suggested in the new model of influenza hemagglutinin-mediated membrane fusion by Bonnafous and Stegmann [43]. In principle, our data on the HIV-1 FP would support the existence of such structures in the target membranes. Formation of those lytic aggregates may precede the formation of gp41 complexes, with interfacially located extended structures. Peptide aggregates interacting superficially with the target membrane at the point of fusion might promote distortion of the external monolayer [16,44]. This target-membrane perturbation would be localized at the fusion point and might be absorbed by the virion membrane closely apposed by the action of the ''hairpin'' structure. In this view, the FP would play an active role in the fusion process mediated by HIV-1 gp41.

Acknowledgements

A.S.C. was a recipient of a predoctoral fellowship of the Basque Government. This work was supported by DGCYT (grant PB96/0171), the Basque Government (PI-1998-32; PI-1999-7) and the University of the Basque Country (UPV-13552/2001).

References

[1] W.R. Gallaher, Cell 50 (1987) 327–328.
[2] M. Rafalski, J. Lear, W. DeGrado, Biochemistry 29 (1990) 7917–7922.
[3] R.W. Doms, J.P. Moore, J. Cell Biol. 151 (2000) F9–F13.
[4] D.M. Eckert, P.S. Kim, Annu. Rev. Biochem. 70 (2001) 777–810.
[5] M.L. Bosch, P.L. Earl, K. Fargnoli, S. Picciafuoco, F. Giombini, F. Wong-Staal, G. Franchini, Science 244 (1989) 694–697.
[6] E.O. Freed, D.J. Myers, R. Risser, Proc. Natl. Acad. Sci. U. S. A. 87 (1990) 4650–4654.
[7] E.O. Freed, E.L. Delwart, G.L. Buchschacher, A.T. Panganiban, Proc. Natl. Acad. Sci. U. S. A. 89 (1992) 70–74.
[8] S.R. Durell, I. Martin, J. Ruysschaert, Y. Shai, R. Blumenthal, Mol. Membr. Biol. 14 (1997) 97–112.
[9] S. Nir, J.L. Nieva, Prog. Lipid Res. 39 (2000) 181–206.
[10] X. Han, L.K. Tamm, Biosci. Rep. 20 (2000) 501–518.
[11] D. Chan, P.S. Kim, Cell 93 (1998) 681–684.
[12] J. Yang, C.M. Gabrys, D.P. Weliky, Biochemistry 40 (2001) 8126–8137.
[13] J.L. Nieva, S. Nir, A. Muga, F.M. Goñi, J. Wilschut, Biochemistry 33 (1994) 3201–3209.
[14] F.B. Pereira, F.M. Goñi, J.L. Nieva, FEBS Lett. 362 (1995) 243–246.
[15] F.B. Pereira, F.M. Goñi, A. Muga, J.L. Nieva, Biophys. J. 73 (1997) 1977–1986.
[16] A. Agirre, C. Flach, F.M. Goñi, R. Mendelsohn, J.M. Valpuesta, F. Wu, J.L. Nieva, Biochim. Biophys. Acta 1467 (2000) 153–164.
[17] M.J. Hope, M.B. Bally, G. Webb, P.R. Cullis, Biochim. Biophys. Acta 812 (1985) 55–65.
[18] C.S.F. Böttcher, C.M. van Gent, C. Fries, Anal. Chim. Acta 24 (1961) 203–204.
[19] H. Ellens, J. Bentz, F.C. Szoka, Biochemistry 24 (1985) 3099–3106.
[20] J.C. McIntyre, R. Sleight, Biochemistry 30 (1991) 11819–11827.
[21] D.K. Struck, D. Hoekstra, R.E. Pagano, Biochemistry 20 (1981) 4093–4099.
[22] M.B. Ruiz-Argüello, F.M. Goñi, F.B Pereira, J.L. Nieva, J. Virol. 72 (1998) 1775–1781.
[23] M. Jelokhani-Niaraki, K. Nakashima, H. Kodama, M. Kondo, J. Biochem. 123 (1998) 790–797.
[24] L. Stryer, Annu. Rev. Biochem. 47 (1978) 819–846.
[25] J.L.R. Arrondo, A. Muga, J. Castresana, C. Bernabeu, F.M. Goñi, FEBS Lett. 252 (1989) 118–120.
[26] I. Muñoz-Barroso, S. Durell, K. Sakaguchi, E. Appella, R. Blumenthal, J. Cell Biol. 140 (1998) 315–323.
[27] P.W. Mobley, A.J. Waring, M.A. Sherman, L.M. Gordon, Biochim. Biophys. Acta 1418 (1999) 1–18.
[28] R.A. Dluhy, D.G. Cameron, H.H. Mantsch, R. Mendelshon, Biochemistry 22 (1983) 6318–6325.
[29] H.L. Casal, H.H. Mantsch, F. Paltauf, H. Hauser, Biochim. Biophys. Acta 919 (1987) 275–286.
[30] H.L. Casal, A. Martin, H.H. Mantsch, F. Paltauf, H. Hauser, Biochemistry 26 (1987) 7395–7401.
[31] A. Blume, W. Hübner, G. Messner, Biochemistry 27 (1988) 8239–8249.
[32] G. Basáñez, F.M. Goñi, A. Alonso, FEBS Lett. 411 (1997) 281–286.
[33] J.M.M. Caaveiro, A. Molina, P. Rodríguez-Palenzuela, F.M. Goñi, J.M. González-Mañas, Protein Sci. 7 (1998) 2567–2577.
[34] O. Tirosh, Y. Barenholz, J. Katzhendler, A. Priev, Biophys. J. 74 (1998) 1371–1379.
[35] J.L. Nieva, S. Nir, J. Wilschut, J. Liposome Res. 8 (1998) 165–182.
[36] G.E. Gilbert, B.C. Furie, B. Furie, J. Biol. Chem. 265 (1990) 815–822.
[37] W.L.C. Vaz, G. Schoellmann, Biochim. Biophys. Acta 439 (1976) 206–218.
[38] L.M. Gordon, C. Curtain, Y.C. Zhong, A. Kirkpatrick, P. Mobley, A.J. Waring, Biochim. Biophys. Acta 1139 (1992) 257–274.
[39] J. Wilschut, in: J. Wilschut, D. Hoekstra (Eds.), Membrane Fusion, Marcel Dekker, New York, 1990, pp. 89–126.
[40] J.M. Seddon, Biochim. Biophys. Acta 1031 (1990) 1–69.
[41] A. Alonso, F.M. Goñi, J.T. Buckley, Biochemistry 39 (2000) 14019–14024.
[42] R.A. Demel, F. Paltauf, H. Hauser, Biochemistry 26 (1987) 8659–8665.
[43] P. Bonnafous, T. Stegmann, J. Biol. Chem. 275 (2000) 6160–6166.
[44] H. Heerklotz, Biophys. J. 81 (2001) 184–195.